PHYSICAL REVIEW C **91**, 061303(R) (2015)

Spectroscopy of ^{76}Se: Prolate-to-oblate shape transition

C. Xu,[1] X. Q. Li,[1] J. Meng,[1] S. Q. Zhang,[1,*] H. Hua,[1,†] S. Y. Wang,[2] B. Qi,[2] C. Liu,[2] Z. G. Xiao,[3,4] H. J. Li,[3] L. H. Zhu,[5] Z. Shi,[5] Z. H. Li,[1] Y. L. Ye,[1] D. X. Jiang,[1] J. J. Sun,[1] Z. H. Zhang,[1] Y. Shi,[1] P. W. Zhao,[1] Q. B. Chen,[1] W. Y. Liang,[1] R. Han,[1] C. Y. Niu,[1] C. G. Li,[1] C. G. Wang,[1] Z. H. Li,[1] S. M. Wyngaardt,[6] R. A. Bark,[7] P. Papka,[6] T. D. Bucher,[6,7] A. Kamblawe,[6,7] E. Khaleel,[6,7] N. Khumalo,[7,8,9] E. A. Lawrie,[7] J. J. Lawrie,[7] P. Jones,[7] S. M. Mullins,[7] S. Murray,[7] M. Wiedeking,[7] J. F. Sharpey-Schafer,[7,8] S. N. T. Majola,[7,10] J. Ndayishimye,[6,7] D. Negi,[7] S. P. Noncolela,[7,8] S. S. Ntshangase,[9] O. Shirinda,[7] P. Sithole,[7,8] M. A. Stankiewicz,[7,10] J. N. Orce,[8] T. Dinoko,[7,8] J. Easton,[7,8] B. M. Nyakó,[11] and K. Juhász[12]

[1]*School of Physics and State Key Laboratory of Nuclear Physics and Technology, Peking University, Beijing 100871, China*
[2]*Shandong Provincial Key Laboratory of Optical Astronomy and Solar-Terrestrial Environment, School of Space Science and Physics, Shandong University, Weihai 264209, China*
[3]*Department of Physics, Tsinghua University, Beijing 100084, China*
[4]*Collaborative Innovation Center of Quantum Matter, Beijing 100084, China*
[5]*School of Physics and Nuclear Energy Engineering, Beihang University, Beijing 100191, China*
[6]*Department of Physics, University of Stellenbosch, Matieland 7602, South Africa*
[7]*iThemba LABS, 7129 Somerset West, South Africa*
[8]*Department of Physics, University of the Western Cape, P/B X17 Bellville 7535, South Africa*
[9]*Department of Physics, University of Zululand, Private Bag X1001, KwaDlangezwa 3886, South Africa*
[10]*Department of Physics, University of Cape Town, Rondebosch 7700, South Africa*
[11]*Institute of Nuclear Research of the Hungarian Academy of Sciences (ATOMKI), H-4001 Debrecen, P.O. Box: 51, Hungary*
[12]*Department of Information Technology, University of Debrecen, Egyetem tér 1, Debrecen, Hungary*

(Received 5 May 2015; revised manuscript received 26 May 2015; published 22 June 2015)

The spectroscopy of ^{76}Se has been studied using the ^{70}Zn(^{12}C, α2n)^{76}Se fusion evaporation reaction. The yrast band of ^{76}Se has been extended to substantially higher spin, allowing observation of the second band crossing. The much-delayed $g_{9/2}$ proton-pair alignment is discussed in terms of the cranked shell model and most likely is caused by a shape transition from prolate to oblate along the yrast line occurring in ^{76}Se. Based on the systematic investigation of the band crossings associated with the $g_{9/2}$ quasiparticle alignments and their relationships with the shape evolutions in the even-A Se and Kr isotopes, a comprehensive picture of shape evolution along with spin and isospin in these nuclei is obtained.

DOI: 10.1103/PhysRevC.91.061303 PACS number(s): 21.10.Re, 23.20.Lv, 27.50.+e

The nuclear shape that reflects the spatial distribution of the nucleons is a fundamental characteristic of the nucleus. For the neutron-deficient Kr and Se nuclei in the $A \sim 70$ mass region, due to the large subshell gaps around Fermi surfaces in the single-particle spectra at prolate and/or oblate deformation for proton and neutron numbers 34, 36, and 38, they exhibit rich and varied shape-related phenomena, such as rapid shape transition, shape coexistence, and triaxiality, and have been the focus of intense theoretical and experimental investigations in recent years.

For the neutron-deficient Kr isotopes, a clear and coherent picture of shape transitions and shape coexistence has been obtained. With the increase of isospin, both the experimental results [1–6] and theoretical calculations [7–14] have demonstrated that the shape transition of the ground state from oblate to prolate occurs at ^{74}Kr. Meanwhile, the coexistence of prolate and oblate shapes has also been discovered in these transitional Kr isotopes. For example, a low-lying prolate deformed excited 0^+ state, which coexists with the oblate 0^+ ground state, has been found in ^{72}Kr [3,15], while low-lying oblate deformed excited 0^+ states, which coexist with the prolate 0^+ ground states, have been found in ^{74,76}Kr [2,5,16–19]. These two coexistent shapes, prolate and oblate, interchange their roles between ^{72}Kr and ^{74}Kr. In addition, with the increase of angular momentum, a rapid shape transition from oblate to prolate along the yrast line has been suggested to occur at very low spins in ^{72}Kr with the recent lifetime measurement [6]. In contrast, the g-factor [20] and lifetime [21] measurements, as well as the excited Vampir calculations [9], indicated that ^{78} Kr undergoes a prolate-to-oblate shape transition along the yrast line. For ^{74,76}Kr, along the yrast line, the prolate shapes of their ground states were found to be relatively stable and persist to higher spins [19,22–26].

Compared to the neutron-deficient Kr isotopes, the situation for the neutron-deficient Se isotopes is not that clear. The early Coulomb excitation experiments in the late 1970s have shown that all the ground states of ^{74,76,78,80,82}Se have prolate shapes [27,28], while the ^{68}Se was found to have an oblate ground state [29,30]. For ^{70,72}Se, total-Routhian-surface [31] and excited Vampir [32] calculations predicted an oblate ground state. In contrast to the predictions, a Coulomb excitation experiment of ^{70}Se suggested its ground state has a prolate shape like the heavier Se isotopes [33]. Later, new lifetime measurements for ^{70,72}Se [34] revised the conclusions drawn from the Coulomb excitation of ^{70}Se. The experimental results in Ref. [34] seem to favor a positive value of the

*sqzhang@pku.edu.cn
†hhua@pku.edu.cn

 ©2015 American Physical Society

spectroscopic quadrupole moment, i.e., oblate shape, for the ^{70}Se. However, due to the large uncertainty of the Coulomb excitation cross section and its relatively weak dependence on the quadrupole moment, in Ref. [34], a precise determination of sign of the quadrupole moment for ^{70}Se was not achieved. More accurate experimental confirmation of exact location where shape transitions of the ground state from oblate to prolate occur in Se isotopes is still needed. Meanwhile, similar to ^{72}Kr, both ^{70}Se and ^{72}Se were found to have a prolate shape at low spins as indicated by the lifetime measurements [34] and the high-spin studies [31]. For ^{74}Se, although direct quadrupole moments measurements have not been made for excited states above the 2^+ level, a high-spin study has revealed that a prolate shape is necessary to reproduce the character of the observed band crossings [35]. As a neighboring nucleus of ^{74}Se, ^{76}Se is also suggested to have a prolate ground state [27]. So far the high-spin structure of ^{76}Se has not been well established and the yrast band was observed only up to spin 12^+ [36]. Due to little experimental information on the high-spin structure, no definite conclusion of shape evolution along the yrast line in ^{76}Se has been drawn. An interesting question therefore arose whether the prolate shape of the ground state in ^{76}Se persists to high spins as in the neighboring isotope ^{74}Se or undergoes a prolate-to-oblate shape transition along the yrast line as in the neighboring isotone ^{78}Kr. To answer this question and to get a complete picture of shape evolution with spin and isospin in the neutron-deficient Se isotopes, extending the high-spin spectroscopic study to ^{76}Se is very meaningful.

Here, we report an experimental investigation on the high-spin properties of ^{76}Se via the ^{70}Zn(^{12}C, α2n)^{76}Se fusion-evaporation reaction. The collective structure of ^{76}Se is expanded significantly, allowing the observation of the second band crossing. The characters of band crossings in ^{76}Se are discussed in terms of the cranked shell model (CSM) and suggest that a possible shape transition from prolate to oblate along the yrast line occurs in ^{76}Se.

The present experiment was performed at iThemba LABS in South Africa. The high-spin states of ^{76}Se were populated via the ^{70}Zn(^{12}C, α2n)^{76}Se fusion-evaporation reaction at beam energies of 60 and 65 MeV. The target was self-supporting ^{70}Zn with a thickness of 0.85 mg/cm^2. The in-beam γ-rays were detected by the AFRODITE array [37], which consists of eight Compton-suppressed clover detectors. The clover detectors have been arranged in two rings at 90° (four clovers) and 135° (four clovers) with respect to the beam direction. To select specific reaction channels, the DIAMANT array [38,39], which consisted of 64 CsI(Tl) scintillators in the present experiment, was also used with the AFRODITE array.

A total of 1.24×10^8 α-γ-γ coincident events were collected, from which a symmetric matrix was built. The level scheme analysis was performed using the RADWARE program [40]. The γ-ray spectra gated on the known γ-ray transitions in ^{76}Se are shown in Fig. 1. In order to obtain Directional Correlations of γ rays deexciting Oriented states (DCO) intensity ratios to determine the multipolarities of γ-ray transitions, the detectors around 90° with respect to the beam direction were sorted against the detectors around 135° to produce a two-dimensional angular correlation matrix. To get clean DCO values for transitions in ^{76}Se, gates were set on uncontaminated stretched E2 transitions. In general, stretched quadrupole transitions were adopted if DCO ratios were larger

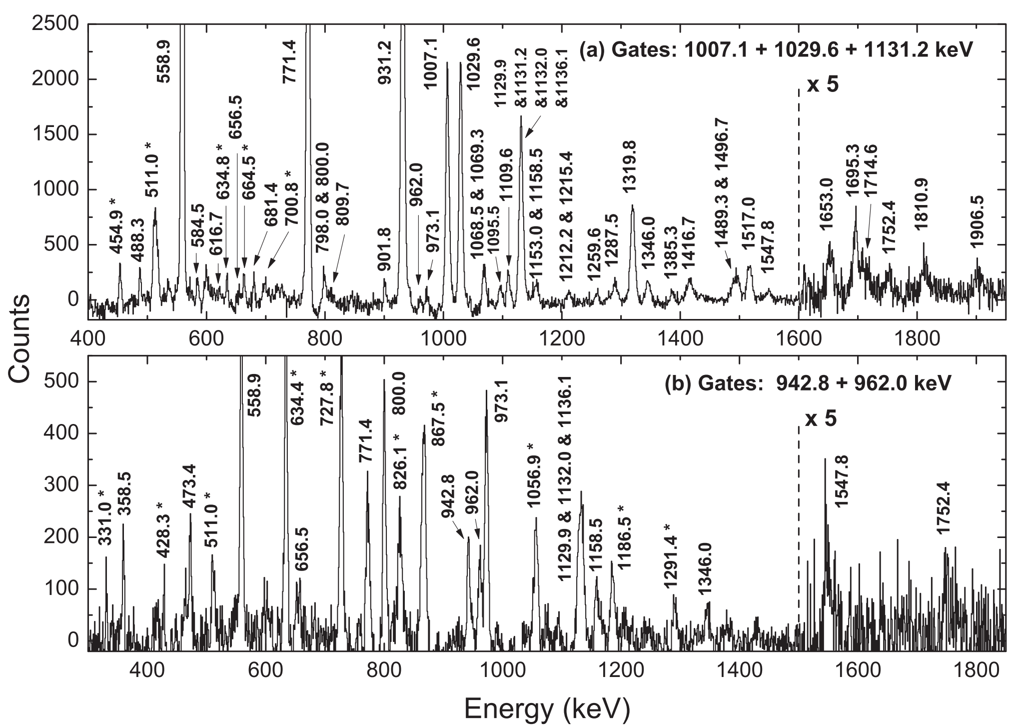

FIG. 1. Coincidence γ-ray spectra generated from (a) the sum of gates on 1007.1-, 1029.6-, and 1131.2-keV transitions, (b) the sum of gates on 942.8- and 962.0-keV transitions. The peaks marked with stars are known contaminants.

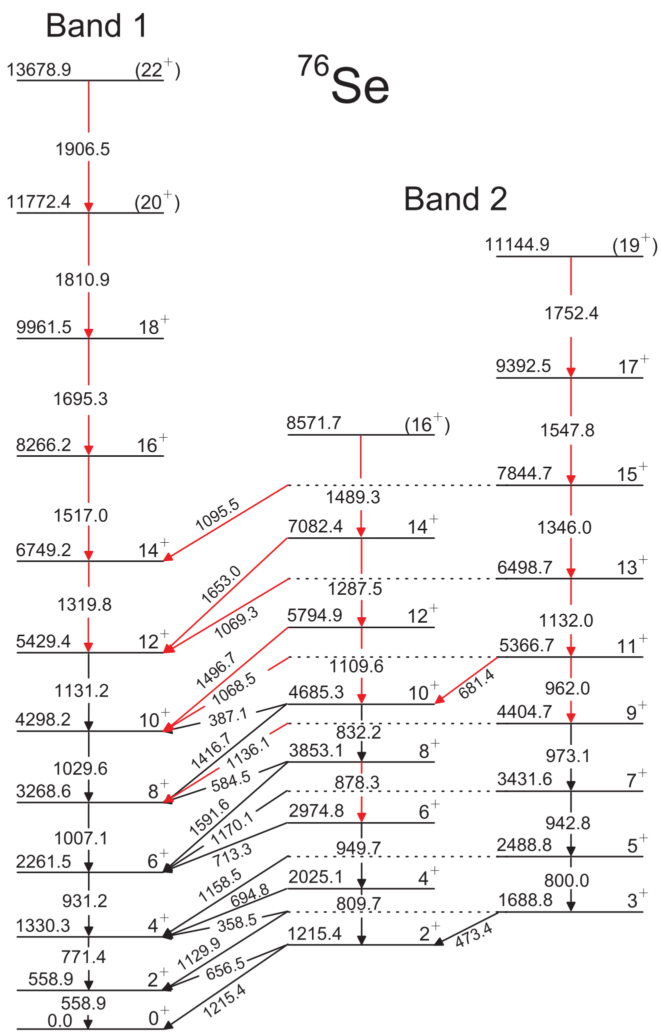

FIG. 2. (Color online) Partial level scheme of ^{76}Se. Energies are in keV. New observed transitions are indicated by red lines.

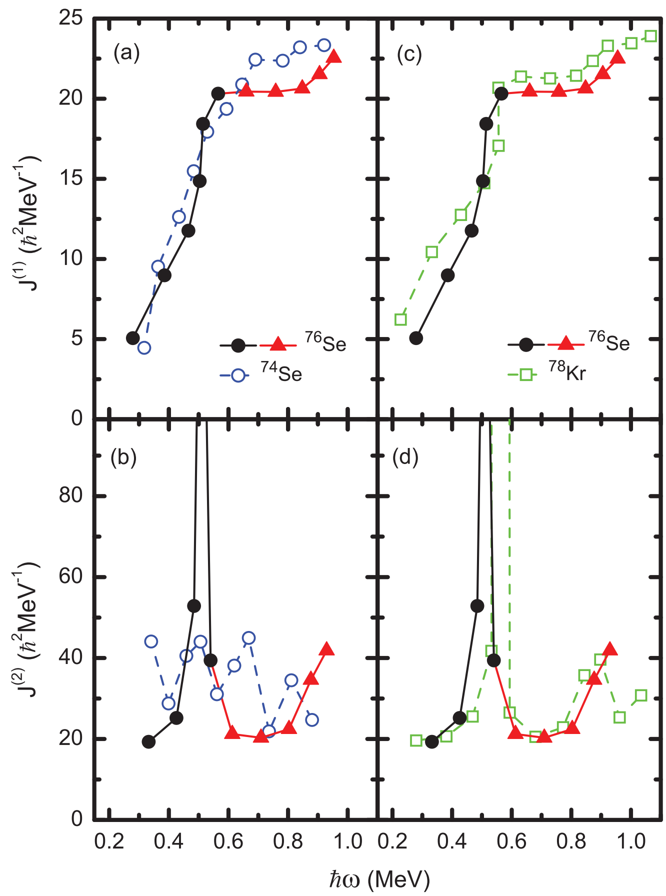

FIG. 3. (Color online) The kinematic $J^{(1)}$ and dynamic $J^{(2)}$ moments of inertia as functions of rotational frequency for the yrast bands in ^{74}Se, ^{76}Se, and ^{78}Kr. New data of ^{76}Se are indicated by solid red triangles.

than 1.0, and stretched dipole transitions were assumed if DCO ratios were less than 0.8.

The partial level scheme of ^{76}Se deduced from the present work is shown in Fig. 2. It was constructed from γ-γ coincidence relationships, intensity balances, and DCO analyses. As shown in Fig. 2, the previously reported positive-parity bands [41,42] have been considerably extended. The yrast band (band 1) of ^{76}Se is extended from spin 12^+ at 5429.4 keV to spin 22^+ at 13678.9 keV and the γ-vibrational band (band 2) is extended from spin 10^+ at 4685.3 keV to spin 19^+ at 11144.9 keV.

The high spin states of ^{76}Se, observed in the present work, allow band crossing phenomena and shape evolution to be studied. In neutron-deficient nuclei in the $A \sim 70$ region, both protons and neutrons occupy the same high-j $g_{9/2}$ intruder subshell and give rise to strong competition between the $g_{9/2}$ neutron and proton alignments, which together with the variety of shapes in these nuclei, means it is usually difficult to discern which alignment will be favored for the band crossing. To identify the origin of the observed band crossings in this mass region, systematics and theoretical studies of the characters of the band crossings are very helpful. In Fig. 3, the kinematic $J^{(1)}$ and dynamic $J^{(2)}$ moments of inertia as functions of rotational frequency for the yrast band in ^{76}Se, in comparison with those for the yrast bands in neighboring isotope ^{74}Se and isotone ^{78}Kr, are plotted.

As shown in Figs. 3(a) and 3(c), at low rotational frequency $<$0.55 MeV, the kinematic moments of inertia for ^{74}Se, ^{76}Se, and ^{78}Kr increase rapidly. Above a rotational frequency of 0.55 MeV, the kinematic moments of inertia of ^{76}Se and ^{78}Kr become flat until a rotational frequency of 0.80 MeV, while the kinematic moment of inertia of ^{74}Se continues to increase until a rotational frequency of 0.70 MeV and then becomes relatively flat. Above the rotational frequency of 0.80 MeV, both ^{76}Se and ^{78}Kr display a similar onset of other upbending. As shown in Fig. 3(b), corresponding to the long upbending in the kinematic moments of inertia, there are two close peaks around frequencies of 0.50 and 0.65 MeV, in the dynamic moment of inertia of the yrast band in ^{74}Se. In Ref. [35], the long upbending observed in ^{74}Se was ascribed to the successive alignments of a pair of $g_{9/2}$ protons around $\hbar\omega = 0.50$ MeV and a pair of $g_{9/2}$ neutrons around $\hbar\omega = 0.65$ MeV, meanwhile its prolate shape was assumed to persist up to the second band crossing region. For ^{78}Kr, the g-factor [20] and lifetime [21]

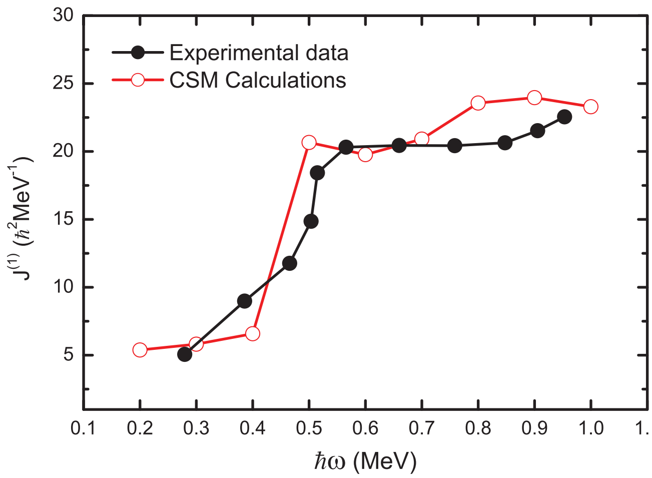

FIG. 4. (Color online) Experimental and calculated moments of inertia for the yrast band of ^{76}Se.

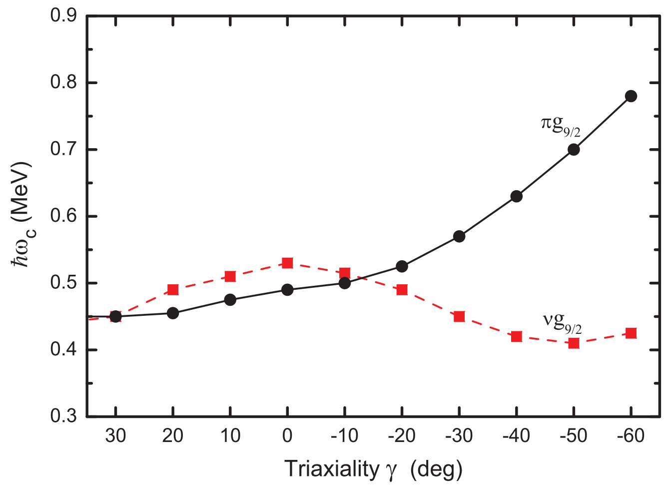

FIG. 5. (Color online) Calculated crossing frequency, $\hbar\omega_c$, for the yrast band as a function of the triaxiality parameter γ for the fixed quadrupole and hexadecapole deformation parameters $\beta_2 = 0.267$ and $\beta_4 = 0.014$.

measurements have indicated that the two well-separated band crossings occurring around $\hbar\omega = 0.55$ and 0.90 MeV can be well ascribed to the alignments of a pair of $g_{9/2}$ neutrons and a pair of $g_{9/2}$ protons, respectively. Meanwhile, a shape transition from prolate to oblate around the first band crossing region for ^{78}Kr is suggested. The striking similarity in the moments of inertia between ^{76}Se and ^{78}Kr indicates that ^{76}Se has a similar alignment behavior to that of isotone ^{78}Kr, which is different from that of isotope ^{74}Se. In addition, it is well known that the nuclear moment of inertia is very sensitive to the nuclear shape. Considering that previous experimental investigations [27,28,43,44] have indicated that all the ground states of ^{74}Se, ^{76}Se, and ^{78}Kr have similar prolate shapes, the similar moment of inertia behavior between ^{76}Se and ^{78}Kr implies that ^{76}Se may undergo a similar prolate-to-oblate shape evolution along the yrast line as ^{78}Kr.

To further understand the details of band-crossing phenomena and shape evolution in ^{76}Se, the CSM calculations [7,45–47] using a Woods-Saxon potential with the deformation parameters $(\beta_2,\beta_4,\gamma) = (0.267,0.014,0^\circ)$ and $(\beta_2,\beta_4,\gamma) = (0.267,0.014,-60^\circ)$ for both quasineutrons and quasiprotons in ^{76}Se are performed. The quadrupole and hexadecapole deformation parameters $\beta_2 = 0.267$ and $\beta_4 = 0.014$ are deduced from the coupled-channel analyses of the polarized-protons inelastic scattering measurements [48]. With the prolate shape, the $g_{9/2}$ proton-pair alignment and $g_{9/2}$ neutron-pair alignment occur around the similar rotational frequency, while with the oblate shape, the band crossing shifts to a much higher rotational frequency for the $g_{9/2}$ proton-pair alignment but remains nearly unchanged for the $g_{9/2}$ neutron-pair alignment. In Fig. 4, we compare the experimental moments of inertia with the theoretical results using the oblate deformation parameters for the yrast band of ^{76}Se. The overall agreements between the experimental data and theoretical results are reasonable. Therefore, the pronounced delay of the $g_{9/2}$ proton-pair alignment can be seen as a sign of oblate shape, and a prolate-to-oblate shape transition along the yrast line appears to well explain the underlying reason for the observation of the delayed band crossing for the $g_{9/2}$ proton-pair alignment in ^{76}Se.

As is well known, triaxiality plays an important role in this transitional nuclear region [11,49–51]. To investigate the dependence of the $g_{9/2}$ quasiparticle crossing frequencies on the triaxiality, in Fig. 5, the calculated $g_{9/2}$ quasineutron and $g_{9/2}$ quasiproton crossing frequencies as functions of the triaxial deformed parameter γ are plotted. Here the Lund convention for the γ value is used in the CSM [52]. It can be seen that with a prolate-like deformation $(-20^\circ < \gamma < 30^\circ)$, the $g_{9/2}$ quasineutron and $g_{9/2}$ quasiproton crossing frequencies are close to each other, while with an oblate-like deformation $(-60^\circ < \gamma < -40^\circ)$, the $g_{9/2}$ quasiproton crossing frequency is much higher than that of $g_{9/2}$ quasineutron. The calculations further illustrate the role of oblate shape for the delayed second band crossing in ^{76}Se.

With the new results in ^{76}Se, to achieve an overall picture of the $g_{9/2}$ quasiparticle alignments and their relationships with the shape evolutions in $A \sim 70$ mass region, the systematics of the $g_{9/2}$ neutron and proton crossing frequencies are plotted as functions of neutron number for even-A Se and Kr isotopes, in Fig. 6. Several interesting systematical features can be clearly seen. (1) For the lighter ^{70,72}Se and ^{72,74,76}Kr isotopes, they have similar alignment schemes: simultaneous $g_{9/2}$ proton-pair and neutron-pair alignments. The ^{72}Kr has been found to have an oblate ground state and undergo a rapid shape evolution from oblate to prolate at low spins. For ^{70,72}Se, previous studies have shown that these two isotopes also have prolate shapes at low spins, although the shapes of their ground states have not been definitely determined. Meanwhile, the prolate shapes of ground states of ^{74,76}Kr were found to be preserved to higher spins. Thus the simultaneous occurrence of $g_{9/2}$ proton-pair and neutron-pair alignments in these light Se and Kr isotopes can be interpreted in terms of their prolate shapes at the band crossing region. (2) For ^{74} Se, the alignment behavior is somewhat different from that of ^{70,72}Se and ^{72,74,76}Kr. The frequency of $g_{9/2}$ quasiproton alignment

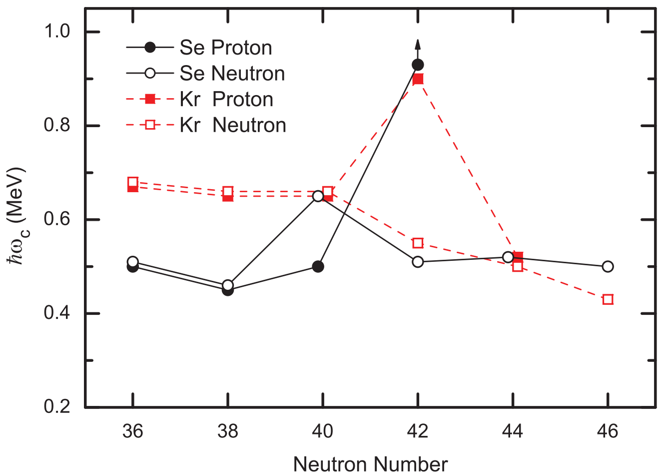

FIG. 6. (Color online) Systematics of experimental crossing frequencies for the $g_{9/2}$ proton-pair and $g_{9/2}$ neutron-pair alignments in the (a) Se and (b) Kr isotopes. The arrow indicates that only the lower limit can be deduced from the present data. Experimental data are taken from Refs. [24,26,31,35,53–59].

is 0.15 MeV lower than that of $g_{9/2}$ quasineutron. Based on the measured $B(E2)$ value, an average prolate quadrupole deformation $\beta_2 = 0.30$ at the band crossing was deduced for ^{74}Se [35]. The CSM calculations in Ref. [35] have shown that if the prolate quadrupole deformation β_2 of ^{74}Se is larger than 0.25, the $g_{9/2}$ quasiproton alignment will occur before the $g_{9/2}$ quasineutron alignment. (3) For the $N = 42$ isotones ^{76}Se and ^{78}Kr, which have prolate ground states, the $g_{9/2}$ quasiproton crossing frequency is far above the $g_{9/2}$ quasineutron crossing frequency. As discussed above, such a delay of $g_{9/2}$ proton-pair alignment can be well attributed to the shape transition from prolate to oblate along the yrast line in these two isotones. (4) For the heavier nucleus ^{80}Kr, the nearly simultaneous $g_{9/2}$ proton and neutron pair alignments occur again. In Ref. [54], the almost simultaneous alignments of $g_{9/2}$ neutron and proton pairs in ^{80}Kr can be explained by assuming an oblate-to-prolate shape change. In contrast to ^{80}Kr, which has an oblate ground state, the $N = 44$ isotone ^{78}Se was suggested to have a prolate ground state with the Coulomb excitation experiments [27]. So far the yrast band of ^{78}Se was only established up to spin 12^+ and the first band crossing was ascribed to the $g_{9/2}$ neutron-pair alignment. The $g_{9/2}$ proton-pair alignment, which is sensitive to the nuclear shape as discussed, has not been observed in this nucleus. Thus, it would be very interesting to extend the high-spin spectroscopic study to ^{78}Se.

In this paper we reported a spectroscopic study of ^{76}Se. The yrast sequence of ^{76}Se is first extended up to the second band crossing region. Based on the systematic comparison with the band crossings observed in the neighboring nuclei and CSM calculations, the much-delayed alignment of $g_{9/2}$ proton pair most likely is caused by a shape transition from prolate to oblate along the yrast line occurring in ^{76}Se. Systematic study of the underlying reason for the band crossings observed in the Se and Kr isotopes gives a comprehensive picture of the shape evolutions along with spin and isospin in this mass region. To get further insight into the shape evolutions in this mass region, more experimental spectroscopic and theoretical studies are needed; especially in determining the ground-state triaxiality in this region by using, for instance, the technique of rotational invariants [60,61].

ACKNOWLEDGMENTS

This work is support by the Natural Science Foundation of China under Grants No. 11175003, No. 11175108, No. 11235001, No. 11335002, No. 11320101004, No. 11375015, No. 11375017, No. 11079025, No. 11461141001, No. 11461141002, and No. J1103206, the Chinese Major State Basic Research Development Program under Grant No. 2013CB834400, and the SA/CHINA research collaboration in science and technology under Grant No. CS05-L06. The authors thank Dr. Q. W. Fan for making the target and the iThemba LABS technical staff and accelerator group for their support and providing the beam.

[1] G. de Angelis *et al.*, Phys. Lett. B **415**, 217 (1997).
[2] F. Becker *et al.*, Eur. Phys. J. A **4**, 103 (1999).
[3] E. Bouchez *et al.*, Phys. Rev. Lett. **90**, 082502 (2003).
[4] A. Gade *et al.*, Phys. Rev. Lett. **95**, 022502 (2005); **96**, 189901(E) (2006).
[5] E. Clément *et al.*, Phys. Rev. C **75**, 054313 (2007).
[6] H. Iwasaki *et al.*, Phys. Rev. Lett. **112**, 142502 (2014).
[7] W. Nazarewicz *et al.*, Nucl. Phys. A **435**, 397 (1985).
[8] A. Petrovici, K. W. Schmid, and A. Faessler, Nucl. Phys. A **665**, 333 (2000).
[9] A. Petrovici *et al.*, J. Phys. G: Nucl. Part. Phys. **32**, 583 (2006).
[10] M. Bender, P. Bonche, and P.-H. Heenen, Phys. Rev. C **74**, 024312 (2006).
[11] M. Girod *et al.*, Phys. Lett. B **676**, 39 (2009).
[12] P. Möller, A. J. Sierk, R. Bengtsson, H. Sagawa, and T. Ichikawa, Phys. Rev. Lett. **103**, 212501 (2009).
[13] K. Sato and N. Hinohara, Nucl. Phys. A **849**, 53 (2011).
[14] Y. Fu *et al.*, Phys. Rev. C **87**, 054305 (2013).
[15] B. J. Varley *et al.*, Phys. Lett. B **194**, 463 (1987).
[16] R. B. Piercey *et al.*, Phys. Rev. Lett. **47**, 1514 (1981).
[17] C. Chandler *et al.*, Phys. Rev. C **56**, R2924 (1997).
[18] C. Chandler *et al.*, Phys. Rev. C **61**, 044309 (2000).
[19] A. Görgen *et al.*, Eur. Phys. J. A **26**, 153 (2005).
[20] J. Billowes *et al.*, Phys. Rev. C **47**, R917 (1993).
[21] P. K. Joshi *et al.*, Nucl. Phys. A **700**, 59 (2002).
[22] C. J. Gross *et al.*, Nucl. Phys. A **501**, 367 (1989).
[23] S. L. Tabor *et al.*, Phys. Rev. C **41**, 2658 (1990).
[24] J. Heese *et al.*, Phys. Rev. C **43**, R921 (1991).
[25] D. Rudolph *et al.*, Phys. Rev. C **56**, 98 (1997).
[26] J. J. Valiente-Dobón *et al.*, Phys. Rev. C **71**, 034311 (2005).
[27] R. Lecomte *et al.*, Nucl. Phys. A **284**, 123 (1977).
[28] R. Lecomte, S. Landsberger, P. Paradis, and S. Monaro, Phys. Rev. C **18**, 2801 (1978).
[29] S. M. Fischer *et al.*, Phys. Rev. Lett. **84**, 4064 (2000).

[30] A. Obertelli *et al.*, Phys. Rev. C **80**, 031304(R) (2009).
[31] T. Mylaeus *et al.*, J. Phys. G: Nucl. Part. Phys. **15**, L135 (1989).
[32] A. Petrovici, K. W. Schmid, and Amand Faessler, Nucl. Phys. A **728**, 396 (2003).
[33] A. M. Hurst *et al.*, Phys. Rev. Lett. **98**, 072501 (2007).
[34] J. Ljungvall *et al.*, Phys. Rev. Lett. **100**, 102502 (2008).
[35] J. Döring *et al.*, Phys. Rev. C **57**, 2912 (1998).
[36] Evaluated nuclear structure data file, http://www.nndc.bnl.gov/ensdf/.
[37] J. F. Sharpey-Schafer, Nucl. Phys. News **14**, 5 (2004).
[38] J. N. Scheurer *et al.*, Nucl. Instrum. Methods Phys. Res. A **385**, 501 (1997).
[39] J. Gál *et al.*, Nucl. Instrum. Methods Phys. Res. A **516**, 502 (2004).
[40] D. C. Radford, Nucl. Instrum. Methods Phys. Res. A **361**, 297 (1995).
[41] J. C. Wells *et al.*, Phys. Rev. C **22**, 1126 (1980).
[42] T. Matsuzaki and H. Taketani, Nucl. Phys. A **390**, 413 (1982).
[43] A. E. Kavka *et al.*, Nucl. Phys. A **593**, 177 (1995).
[44] F. Becker *et al.*, Nucl. Phys. A **770**, 107 (2006).
[45] S. Cwiok *et al.*, Comput. Phys. Commun. **46**, 379 (1987).
[46] R. Wyss *et al.*, Phys. Lett. B **215**, 211 (1988).
[47] F. R. Xu, W. Satuła, and R. Wyss, Nucl. Phys. A **669**, 119 (2000).
[48] S. Matsuki *et al.*, Phys. Rev. Lett. **51**, 1741 (1983).
[49] W. Andrejtscheff and R. Petkov, Phys. Lett. B **329**, 1 (1994).
[50] S. Y. Wang *et al.*, Phys. Lett. B **703**, 40 (2011).
[51] S. F. Shen, S. J. Zheng, F. R. Xu, and R. Wyss, Phys. Rev. C **84**, 044315 (2011).
[52] G. Andersson *et al.*, Nucl. Phys. A **268**, 205 (1976).
[53] H. Sun *et al.*, Phys. Rev. C **59**, 655 (1999).
[54] G. Mukherjee *et al.*, Phys. Rev. C **64**, 034316 (2001).
[55] N. Yoshinaga, K. Higashiyama, and P. H. Regan, Phys. Rev. C **78**, 044320 (2008).
[56] G. Rainovski *et al.*, J. Phys. G: Nucl. Part. Phys. **28**, 2617 (2002).
[57] R. Schwengner *et al.*, Z. Phys. A **326**, 287 (1987).
[58] S. M. Fischer, C. J. Lister, and D. P. Balamuth, Phys. Rev. C **67**, 064318 (2003).
[59] P. Kemnitz *et al.*, Nucl. Phys. A **425**, 493 (1984).
[60] K. Kumar, Phys. Rev. Lett. **28**, 249 (1972).
[61] D. Cline, Annu. Rev. Nucl. Part. Sci. **36**, 683 (1986).